Thin Solid Films 632 (2017) 73–78

Contents lists available at ScienceDirect

Thin Solid Films

journal homepage: www.elsevier.com/locate/tsf

Solution process for fabrication of thin film CdS/CdTe photovoltaic cell for building integration

Amruta Mutalikdesai, Sheela K. Ramasesha *

Divecha Centre for Climate Change, Indian Institute of Science, Bangalore 560012, India

ARTICLE INFO

Article history:
Received 12 June 2016
Received in revised form 4 April 2017
Accepted 13 April 2017
Available online 23 April 2017

Keywords:
CBD
TiO_2 buffer layer
Semitransparent
CdS/CdTe PV and thin film

ABSTRACT

A low-cost, scalable chalcogenide semiconductor thin film deposition process, Chemical Bath Deposition, is used to fabricate semi-transparent TiO_2/CdS/CdTe solar cells. Cadmium telluride (CdTe) acts as an absorber and cadmium sulphide (CdS) is the window layer with band gaps of 1.45 eV and 2.45 eV, respectively. In this work, about 400 nm thick p-CdTe and ~200 nm n-CdS films are deposited on titanium dioxide (TiO_2) coated substrate. Insertion of TiO_2 layer at front contact between FTO coated glass substrate and CdS; improved CdS/CdTe PV cell performance by reducing the leakage current. This resulted in increase of short circuit current in the device. At the initial stage of development the cell exhibits a voltage of 100.53 mV and photocurrent of 14.7 mA/cm^2, illustrates the potential of the process. The devices are characterized using FE-SEM, UV–Visible spectroscopy, XRD and AFM. The fabricated PV cells are around 43% transparent and these semi-transparent cells can be used as windowpanes for building integrated photovoltaic applications.

1. Introduction

In the present scenario, fossil fuel reserves are not enough to meet the energy requirements of the world. In addition, burning fossil fuels has other detrimental effect of emission of greenhouse gases leading to global warming. Alternative renewable energy sources such as solar and wind can be utilized to overcome the energy deficit. Researchers are working on different technologies to harness these renewable resources in an efficient way because installation of photovoltaic (PV) modules will provide energy with less carbon footprint [1].

For many decades, silicon based solar cells dominated the market and with an increase in manufacturing capabilities, thin film PV cells are gaining significance [2]. Major deposition techniques such as sputtering [3], Metal Organic Chemical Vapor Deposition (MOCVD) [4], Closed Spaced Sublimation (CSS) [5], thermal evaporation [6], e-beam evaporation [7], Molecular Beam Epitaxy (MBE) [8] have been attempted to produce thin film PV. The material cost, energy consumption and technologies used by these sophisticated fabrication techniques make the cells and in turn the panels expensive. The area and number of samples that can be coated is limited in order to produce homogeneous thin film. The Chemical Bath Deposition (CBD) provides a simple and economical way for deposition of thin films. Multiple samples can be deposited at a time. Large area deposition is possible with CBD process and it requires basic instrumental setup. CBD is a solution process used to deposit different metal chalcogenide thin films such as cadmium sulphide (CdS), zinc sulphide (ZnS), copper indium diselenide ($CuInSe_2$), cadmium zinc sulphide (CdZnS) and copper selenide (CuSe). The thin films produced by CBD processes are of high quality are used for photovoltaic, solar selective coatings and optical imaging applications [9].

Recent research and development work on photovoltaic focused on energy preserving and reduction of carbon emission to the atmosphere. Semi-transparent PV windows or skylights are integrated in modern buildings, which ensure daylight utilization along with electricity production [10]. Semi-transparent PV is considered to be one of the sustainable building materials. In this regard, the concept of semi-transparent PV was introduced by creating microscopic apertures in opaque silicon modules [11]. Development of these technically sustainable PV is important to compete with the usage of non-renewable sources for electrification. In this article, an attempt is made to produce semi-transparent PV cells, which can be used in Building Integrated Photo Voltaic (BIPV).

This paper focuses on fabrication of a CdS/CdTe ultra-thin film PV cell with TiO_2 as a buffer layer by the CBD method. The key feature of these PV cells is that both the n- and p-type semiconductors are deposited by solution process. The fabricated cells are semi-transparent and the CBD process has been used to deposit multiple large area thin films in a single experiment unlike the traditional vacuum techniques. Here the attempt has been to prove the concept of making environmentally stable semi-transparent p-n junction based inorganic solar cells. The cell thickness is maintained low in order to achieve transparency. Fluorine doped tin oxide (FTO) is used as a substrate as it has unique properties such as high transparency, good electrical conductivity and

* Corresponding author.
E-mail address: sheela.ramasesha@gmail.com (S.K. Ramasesha).

http://dx.doi.org/10.1016/j.tsf.2017.04.036
0040-6090/

chemical stability at high annealing temperatures [12]. Cadmium telluride, p-type semiconductor with optimum band gap of 1.45 eV acts as the absorber layer. A transparent n-type semiconductor cadmium sulphide is used as the window layer, which has band gap of 2.45 eV. Prior to deposition of p- and n-type semiconductors a thin layer of TiO_2 is spin coated on FTO coated glass substrate. TiO_2 has a wide band gap of 3.2 eV and is an n-type conductor. It is a good electron acceptor and transport material [13]. This property of TiO_2 is useful in transportation of electrons generated due to photovoltaic effect in the cell. The insertion of TiO_2 layer improved CdS/CdTe PV cell performance by reducing the leakage current.

2. Experimental

2.1. Thin film coating

The fluorine doped tin oxide (FTO) coated glass of sheet resistance 10 Ω/sq. purchased from Techinstro was used as the substrate. Substrate was thoroughly cleaned using deionized water, ethanolamine and ethanol. TiO_2 layer was spin coated on cleaned FTO substrate. Titanium isopropoxide, ethanol and hydrochloric acid were used to prepare TiO_2 sol. TiO_2 was spin coated at 2000 rpm for 50 s and samples were annealed at 500 °C for 30 min.

A layer of CdS was deposited on TiO_2 coated FTO substrates by CBD method of thin film deposition. This procedure is well established [14]. The bath solution was prepared by using 2×10^{-3} M cadmium acetate, 5×10^{-3} M thiourea and 2×10^{-2} M ammonium acetate and ammonia. Substrates were inserted into the chemical bath. The deposition was carried out for 60 min. After the deposition the samples were removed and washed with distilled water. CdS coated samples were annealed at 350 °C for 10 min. This procedure was repeated to coat second layer of CdS.

Cadmium telluride was also coated using cost effective CBD method. p-CdTe thin layer was deposited on CdS coated substrate. The optimized procedure is described in our previous work [15]. Cadmium acetate ($Cd(CH_3COO)_2 \cdot 2H_2O$), tellurium dioxide ($TeO_2$), triethanolamine (TEA), ammonia and hydrazine hydrate were used to prepare bath solution. The deposition was carried out for 60 min at 92 °C. The procedure was repeated to deposit two more layers of CdTe. Later the sample was treated with saturated solution of cadmium chloride ($CdCl_2$) in methanol and annealed in air at 400 °C.

2.2. Cell fabrication

The n-TiO_2/n-CdS/p-CdTe thin film PV cell was fabricated by annealing the cell at 400 °C for 1 min. This annealing step results in intermixing of the n- and p-type semiconductors forming $CdTe_xS_{1-x}$ junction region [16]. One more layer of CdTe was deposited on top of the cell to fill up the gaps that might have appeared due to the grain growth at high temperature. Prior to electrode deposition surface of the fabricated PV cell was cleaned thoroughly by ultra-sonication using deionized water. Copper and gold (Cu-Au) alloy electrode was deposited by DC sputtering. Around 5 nm of copper was deposited followed by 20 nm of gold.

J-V measurement was carried out both in dark and under illumination using Tracer-2, 1.5 AM solar simulator with 1 SUN (1000 W/m^2) incident power. Ultra 55 Karl-Zeiss Field emission-scanning electron microscopy (FE-SEM) was used to study the surface morphology of each layer of the thin film. Optical band gap measurements of TiO_2, CdS and CdTe thin films are investigated using Perkin–Elmer Lamda 35 UV–Visible spectrophotometer. The structure and crystal orientation was examined by thin film Rigaku X-ray diffractometer. The atomic force microscopy (AFM) measurements were considered to analyze roughness of the thin films.

3. Result and discussions

The PV cells, thus fabricated were characterized using multiple techniques for crystal structure, morphology and electrical performance.

Thin film X-ray diffraction studies on all the samples were carried out in the 2θ range of 20–90° at grazing angle of 0.5°. The diffraction pattern was identified using JCPDS data. Fig. 1 shows the XRD pattern of FTO substrate, CdS, CdTe and TiO_2 layers. The peaks appearing at 2θ of 23.84 (111), 39.48 (220), 46.62 (311) and 57.11 (400) (JCPDS file no: 650890); 28.14 (200) (JCPDS file no: 89-3011) and 30.57 (200) (JCPDS file no: 65-1047) correspond to the cubic phase of CdTe. The peaks of cubic and hexagonal CdS appeared at 26.58 (111), 43.89 (220) (JCPDS file no: 75-1546) and 24.92 (100) (JCPDS file no: 80-0006), respectively. Anatase TiO_2 peaks are found at 25.18 (101) and 47.89 (200) (JCPDS file no: 21-1272). No impurity peaks were detected in the diffraction pattern.

Fig. 2 shows the SEM images of TiO_2, CdS and CdTe thin layers deposited on FTO substrate.

Fig. 2(A) shows TiO_2 buffer layer deposited on FTO substrate annealed at 500 °C for 30 min. TiO_2 is uniformly covering the substrate without any visible pinholes providing better platform for CdS growth. CdS layer as deposited and after heat treatment at 350 °C for 10 min is shown in Fig. 2(B) & (C), respectively. In CdS thin film it was observed that groups of crystallites clubbed to form grains. As deposited CdTe thin film and $CdCl_2$ treated CdTe after annealing at 400 °C is shown in Fig. 2(D) & (E), respectively. CdTe has densely packed microstructure and $CdCl_2$ treatment resulted in enhanced grain growth. In CBD grown CdTe thin film, annealing is a significant step. During annealing grain boundaries are created and grain growth continues through grain boundary movement. The fabrication involves deposition of multiple layers of CdS and CdTe and multiple annealing steps. High temperature annealing, results in random orientation of grains. In CBD process, nucleation and grain growth can be controlled by changing chemical bath environment (temperature and chemistry of solution). During CdTe deposition, CdTe can diffuse through the pinholes and the grain boundaries present in the CdS layer to get in contact with exposed parts of FTO substrate if buffer layer is absent. This will lead to short circuit in the device leading to reduced cell performance. Hence having the buffer layer of TiO_2 has helped in improved cell performance.

Fig. 3(A) schematically represents the superstrate configuration of the device and 3(B) depicts the cross sectional SEM image of the cell. The total cell thickness was found to be 1.4 μm. The individual layer thickness of FTO, CdS along with TiO_2 and CdTe was found to be 650 nm, 305 nm and 450 nm, respectively. Cross section image confirmed the device thickness and the device fabricated was ultrathin.

Fig. 4 shows the topographical images of FTO substrate, TiO_2, CdS and CdTe layer. The surface roughness was calculated by root mean square values. The roughness of FTO substrate was found to be 63.6 nm and after spin coating TiO_2 layer and annealing at high temperature (500 °C) the surface roughness was found to be 20.4 nm. With deposition of CdS the roughness was 21.3 nm. Roughness of the cell after deposition of CdTe thin film, $CdCl_2$ treatment and subsequent annealing at 400 °C increased slightly to 39.4 nm. As the substrate surface provides nucleation sites for the film growth, surface morphology of the substrate (FTO in this case) used plays important role. It is clear from the AFM images that the FTO used influenced the thin film deposition. This has led to increased shunting problems in the device resulting in reduced open circuit voltage.

The optical absorption response was recorded in the wavelength region of 300–1100 nm. Different layers (CdS and CdTe) can absorb photons from different wavelength region of the solar spectrum. The following equation was used to calculate the band gap values.

$$\alpha(\upsilon)h\upsilon = B\left(h\upsilon - E_{gap}\right)^m \quad (1)$$

where $\alpha(\upsilon)$ is the absorption coefficient, B is a constant, $h\upsilon$ is the incident photon energy, E_{gap} is the optical gap and $m = 1/2$ for best curve

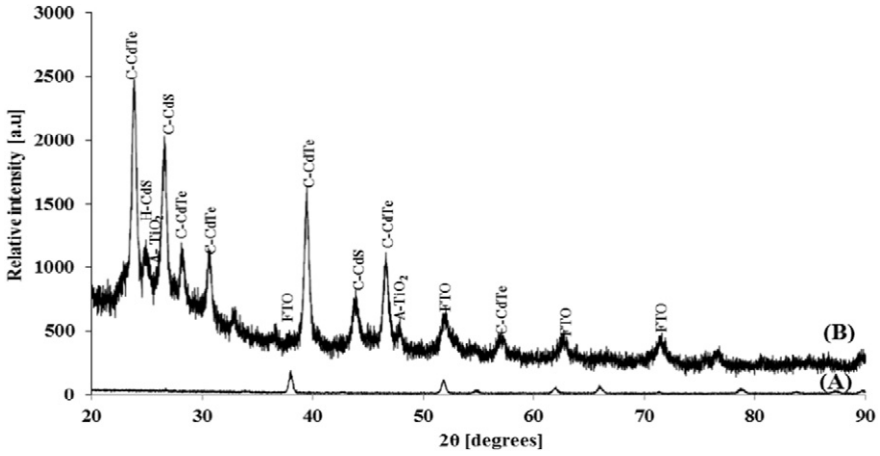

Fig. 1. XRD pattern of (A) FTO substrate and (B) FTO/TiO_2/CdS/CdTe cell annealed at 400°C in air.

fitting of direct allowed transitions. The band gap of TiO_2 is large and it was found to be 3.25 eV. The optical band gap value of CdS was found to be 2.2 eV and that of CdTe was 1.3 eV. Band gap values were obtained by plotting the graph of incident photon energy versus optical gap and extrapolating the straight line portion of the plot to zero which were in good agreement with the literature value [17–19].

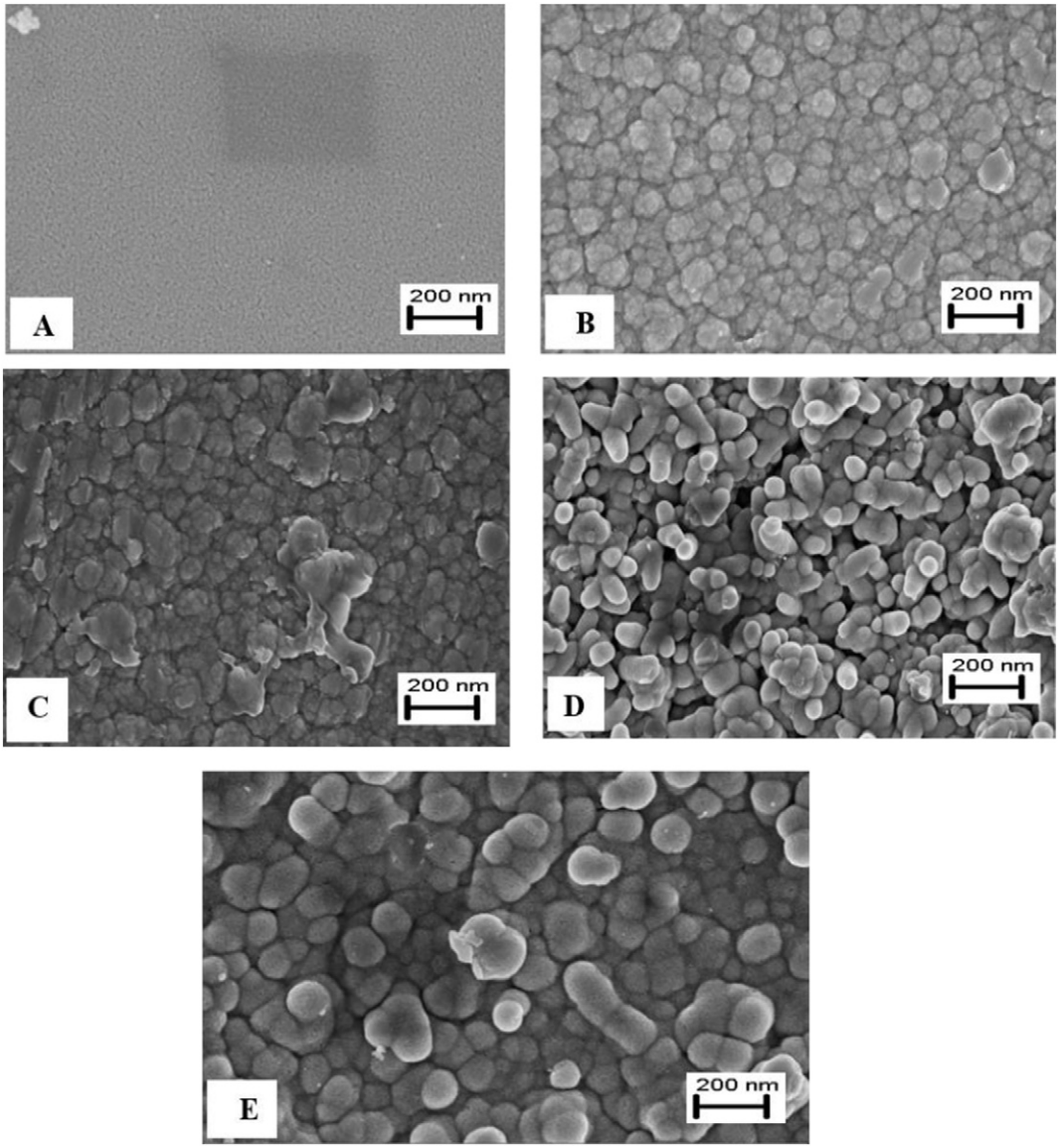

Fig. 2. SEM images of (A) TiO2 layer, (B) CdS as deposited, (C) CdS annealed at 350°C and (D) CdTe as deposited, (E) CdTe annealed at 400°C.

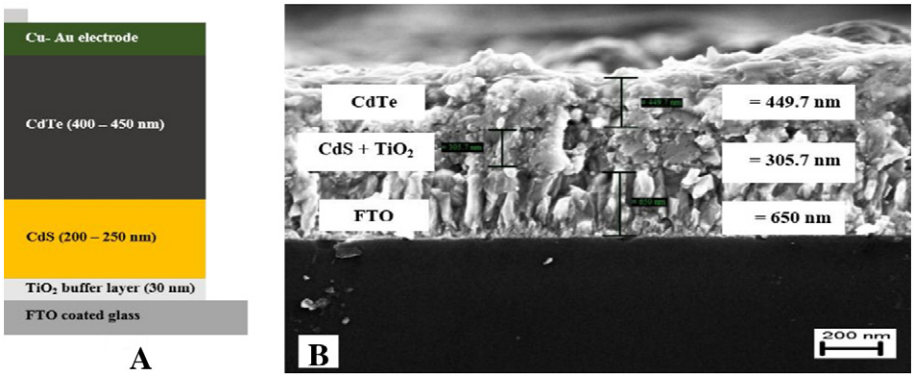

Fig. 3. (A) Device architecture and (B) Cross sectional SEM image of the device.

Fig. 5 shows the transmittance spectra of FTO, after coating TiO_2 and thin films of CdS and CdTe (cell). The fabricated cells are around 43% transparent, which is achieved by reducing the thickness of the cell. Since titania (TiO_2) layer itself absorbs about 30% of the incoming radiation the transparency of the cell is reduced compared to the cell fabricated without TiO_2 layer [20]. The fabricated devices were semi-transparent. These semi-transparent PV cells can replace traditional windowpanes and skylights of buildings. These smart windows act as a screen against UV radiation, in addition to functioning as a normal window and will generate electricity [21].

The photo-current density-voltage (*J-V*) curves of CdS/CdTe PV cell fabricated by CBD method is shown in Fig. 6 (A). Cell performance was measured in both dark and under illumination. The shape of the curve is not a square *J-V* curve exhibited by a typical solar cell. It is known that the shape of the *J-V* curve is a function of the thickness of the absorber layer in the device [22,23]. Few micrometers of CdTe is required to absorb all the photons. A numerical model shows that for 1 μm thick CdTe, photo carrier generation rate decreases by a factor of 0.01 [24]. Since the aim of the paper was to demonstrate the concept of making windowpanes that generate electricity while blocking harmful UV radiation (as seen in Fig. 5), thinner absorber layers are deposited. Thinning of the absorber layer (<1 μm) increases the recombination and affect the cell characteristics. The performance parameters were found to be: open circuit voltage (V_{oc}) of 100.53 mV, short circuit current density (J_{Sc}) of 14.7 mA/cm^2, fill factor (*FF*) of 27.7% and solar energy conversion efficiency of 0.41%. The FF and efficiency (η) was calculated using the equations:

$$FF = \frac{V_{mp} I_{mp}}{V_{oc} I_{sc}} \tag{2}$$

$$\eta = \frac{V_{oc} I_{sc} FF}{P_{in}} \tag{3}$$

where V_{mp} and I_{mp} are voltage and current at maximum power, respectively. P_{in} is input power.

Low V_{oc} and fill factor observed were possibly due to carrier recombination loss near the back contact. Copper when used as a back contact is known to be a fast diffuser in CdTe, especially in thin CdTe cells with thickness <1 μm [25]. Optimization of back contact is under progress to enhance the cell performance.

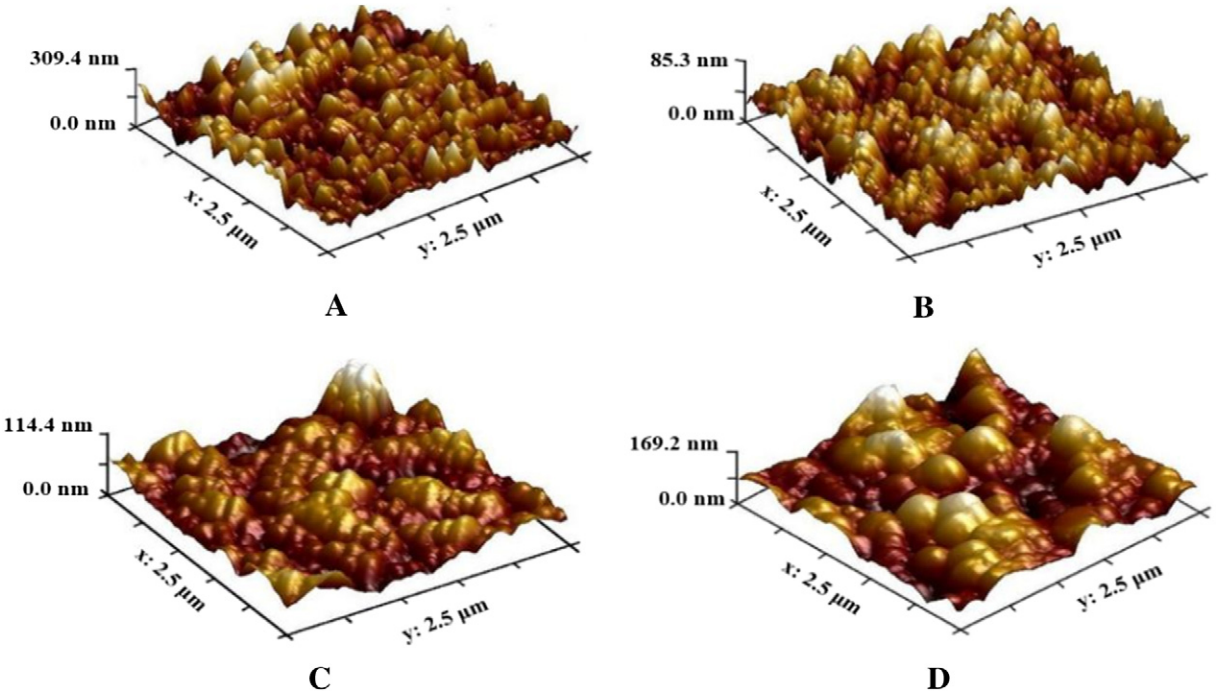

Fig. 4. AFM images: (A) FTO substrate, (B) TiO_2 coated on FTO, (C) CdS thin film, (D) CdTe thin film (CELL).

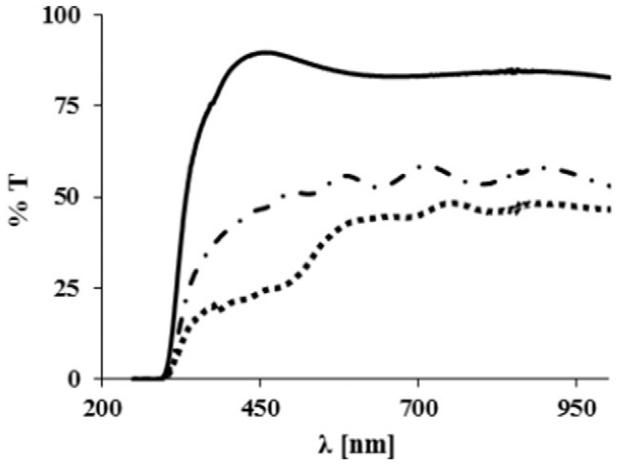

Fig. 5. Transmittance spectra of FTO (solid line), FTO_TiO_2 (dash-dot line) and PV cell (dotted line).

Fig. 6(B) depicts the semi-log plots of the dark and light *J-V* curves. This graph represents the good diode rectifying property of the PV cell under dark conditions. The diode parameter such as dark saturation current and ideality factor under dark condition were calculated using semi log curves and were found to be 7.29×10^{-6} A and 2.09, respectively. Pinholes were not dominant in the thin film PV produced by inexpensive, simple CBD process. As expected the leakage current was reduced and the efficiency of cell was improved compared to earlier work on CdTe/CdS by CBD method [20]. Thus insertion of buffer (TiO_2) layer at the front contact was beneficial. Multiple cells were measured and the recorded cell parameters (V_{oc} and J_{sc}) of each cell are shown in the Fig. 6(C).

Quantum efficiency (QE) measurement reveals the ratio of number of charge carriers collected by PV cell to the number of photons of given energy incident on the cell. Fig. 7 shows the internal (IQE) and external (EQE) quantum efficiency in the wavelength range of 300–1100 nm. To measure QE the light is shined from TCO side, the photo charge carriers generated by the absorption of photons by CdTe is indicated by rise in QE below 1100 nm. The drop in QE at lower wavelength (around 550 nm) shows absorption loss in CdS (window layer). In CdS/CdTe PV cells, CdTe alone is responsible for generation of photo charge carriers and these get separated at the junction. The high energy electrons cross the barrier resistance and diffuse through CdS and get collected at FTO electrode. Simultaneously, holes move towards back contact. The reduced QE at longer wavelengths may be due to inadequate absorption of photons as the absorber layer is ultrathin. To achieve total charge collections, the thickness of the CdTe layer should be >1 μm [24]. The thicker window layer restricts light transmission in

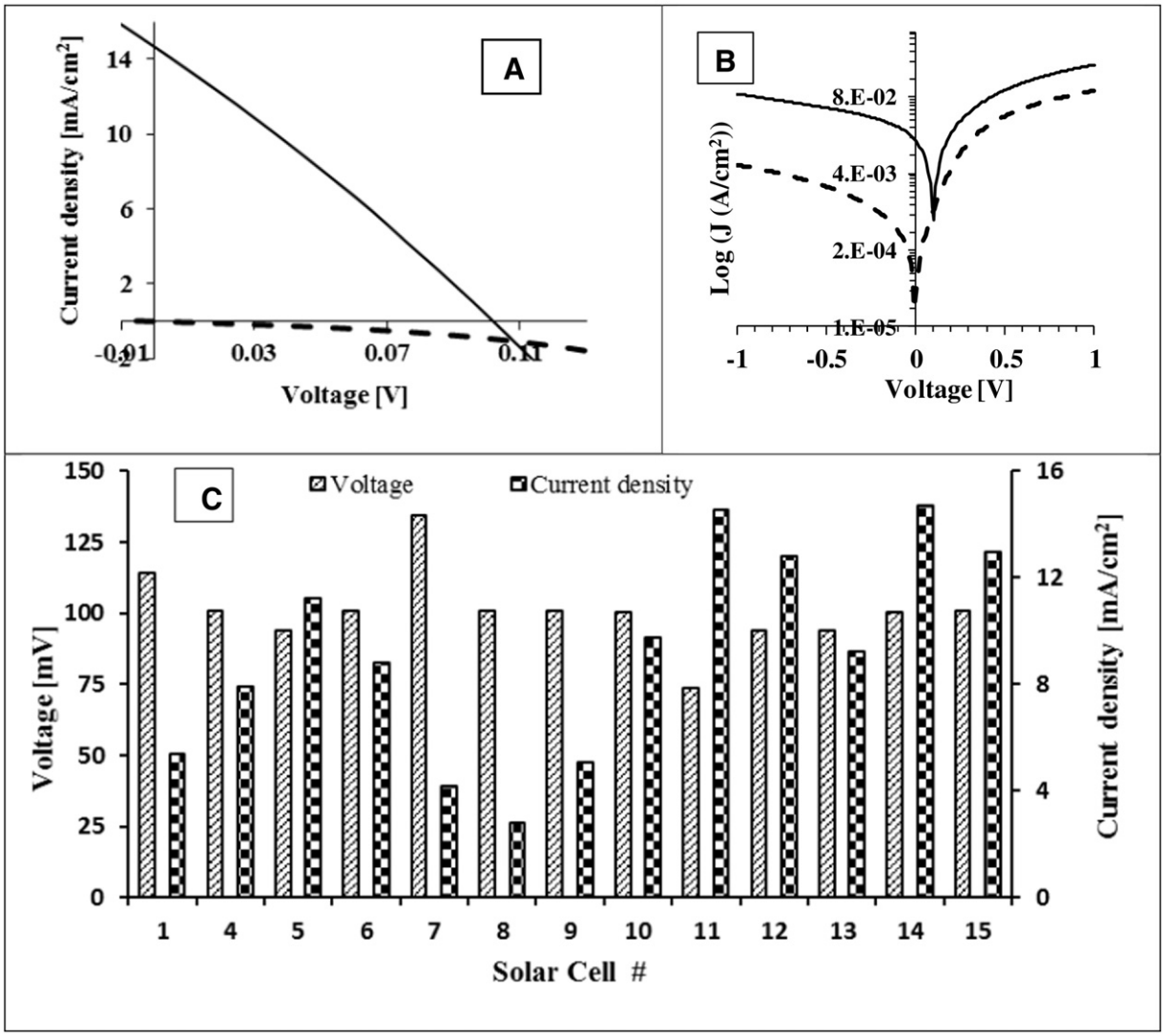

Fig. 6. (A) *J-V* curve of PV cell (B) Semi log plot of dark (broken line) and light curve (solid line) (C) Performance of multiple cells prepared by the CBD process.

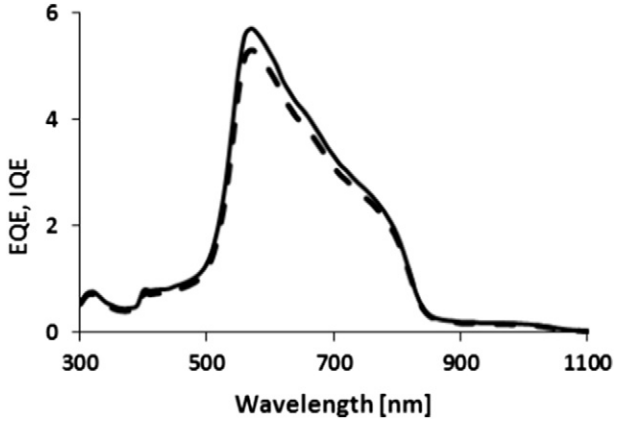

Fig. 7. Spectral quantum efficiency (EQE, IQE) of the TiO_2/CdS/CdTe cell. Solid line and broken line represent IQE and EQE, respectively.

to the absorber layer and in turn contributes to reduction of QE [26]. The ratio of thickness of p- and n-type semiconductors may also be responsible for the observed QE. Electrons with short diffusion lengths generated far from junction may not be collected at the electrode, which could also be the reason for reduced QE. Very rough surface of the TCO may reflect incoming photons and decline photon flux to the absorber layer lowering QE.

4. Conclusion

The proof for developing semi-transparent p-n junction based stable inorganic solar cells for BIPV application is provided. Chemical Bath Deposition offers the possibility of a modest, adaptable process for CdS and CdTe thin film deposition on large areas. A semi-transparent CdS/CdTe photovoltaic cell has been fabricated by cost-effective Chemical Bath Deposition process. Insertion of TiO_2 buffer layer between thin semiconducting layer and front contact is proved to be beneficial. This reduced recombination current between FTO, CdS and CdTe layers. At the present stage of development, J_{sc} of 14.7 mA/cm^2, V_{oc} of 100.53 mV and *FF* of 27.7% is observed. Crystal Structure studies are in good agreement with the structures observed for CdS and CdTe by other deposition techniques. Morphological studies confirmed uniform deposition of the thin films and the fabricated device is indeed ultrathin. It is found that the quantum efficiency of the cell reduced due to thin CdTe layer and recombination at back contact. Efforts are going on to improve the *J-V* characteristics by improving the process further by using less rough TCO and improving deposition technique to reduce the CdS layer thickness. These semi-transparent PV devices have enormous potential to replace traditional windows and skylights of buildings for harnessing solar energy to generate electricity for lighting requirements of the building. This provides a significant contribution in reduction of carbon footprint.

Acknowledgements

We thank Harish Barshilia, P. Chowdhury of NAL, Bangalore for assistance with electrode deposition and Professor K.L. Narasimhan, IIT Bombay, Mumbai for numerous valuable discussions during the course of this work.

References

[1] S. Perry, J. Klemeš, I. Perry, Integrating waste and renewable energy to reduce the carbon footprint of locally integrated energy sectors, Energy 33 (2008) 1489–1497.
[2] S. Hegedus, Thin film solar modules: the low cost, high throughput and versatile alternative to Si wafers, Prog. Photovolt. Res. Appl. 14 (2006) 393–411.
[3] A. Gupta, A.D. Compaan, All-sputtered 14% CdS/CdTe thin-film solar cell with ZnO: Al transparent conducting oxide, Appl. Phys. Lett. 85 (2004) 684–686.
[4] A. Nouhi, R.J. Stirn, P.V. Meyers, C.H. Liu, High-efficiency CdTe thin-film solar cells using metalorganic chemical vapor deposition techniques, J. Vac. Sci. Technol. A 7 (1989) 833–836.
[5] T.L. Chu, S.S. Chu, C. Ferekides, C.Q. Wu, J. Britt, C. Wang, 13.4% efficient thin-film CdS/CdTe solar cells, J. Appl. Phys. 70 (1991) 7608–7612.
[6] S. Chakrabarti, S. Ghosh, S. Chaudhuri, A.K. Pal, Rapid thermal processing for the preparation of CdTe film, J. Phys. D. Appl. Phys. 32 (1989) 1258–1268.
[7] J.P. Mangalhara, R. Thangaraj, O.P. Agnihotri, Structural, optical and photoluminescence properties of electron beam evaporated CdSe1 − xTex films, Sol. Energy Mater. 19 (1989) 157–165.
[8] S. Sivananthan, X. Chu, J. Reno, J.P. Faurie, Relation between crystallographic orientation and the condensation coefficients of Hg, Cd, and Te during molecular-beamepitaxial growth of Hg1-xCdxTe and CdTe, J. Appl. Phys. 60 (1986) 13591363.
[9] R.S. Mane, C.D. Lokhande, Chemical deposition method for metal chalcogenide thin films, Mater. Chem. Phys. 65 (2000) 1–31.
[10] G. Gorgolis, D. Karamanis, Solar energy materials for glazing technologies, Sol. Energy Mater. Sol. Cells 144 (2015) 559–578.
[11] A. Takeoka, S. Kouzuma, H. Tanaka, H. Inoue, K. Murata, M. Morizane, N. Nakamura, H. Nishiwaki, M. Ohnishi, S. Nakano, Y. Kuwano, Development and application of seethrough a-Si solar cells, Sol. Energy Mater. Sol. Cells 29 (1993) 243–252.
[12] H. Bisht, H.-T. Eun, A. Mehrtens, M.A. Aegerter, Comparison of spray pyrolyzed FTO, \ATO\ and \ITO\ coatings for flat and bent glass substrates, Thin Solid Films 351 (1999) 109–114.
[13] J. Li, X. Chen, W. Xu, C.-Y. Nam, Y. Shi, TiO_2 nanofiber solid-state dye sensitized solar cells with thin TiO_2 hole blocking layer prepared by atomic layer deposition, Thin Solid Films 536 (2013) 275–279.
[14] R. Ortega-Borges, D. Lincot, Mechanism of chemical bath deposition of cadmium sulfide thin films in the ammonia-thiourea system in situ kinetic study and modelization, J. Electrochem. Soc. 140 (1993) 3464–3473.
[15] L. Gouda, Y.R. Aniruddha, S.K. Ramasesha, Correlation between the solution chemistry to observed properties of CdTe thin films prepared by CBD method, J. Mod. Phys. 3 (2012) (1870-1877).
[16] T. Takamoto, T. Agui, H. Kurita, M. Ohmori, Improved junction formation procedure for low temperature deposited CdS/CdTe solar cells, Sol. Energy Mater. Sol. Cells 49 (1997) 219–225.
[17] W.-J. Yin, S. Chen, J.-H. Yang, X.-G. Gong, Y. Yan, S.-H. Wei, Effective band gap narrowing of anatase TiO2 by strain along a soft crystal direction, Appl. Phys. Lett. 96 (2010) 221901(1)–221901(3).
[18] J. Han, C. Spanheimer, G. Haindl, G. Fu, V. Krishnakumar, J. Schaffner, C. Fan, K. Zhao, A. Klein, W. Jaegermann, Optimized chemical bath deposited CdS layers for the improvement of CdTe solar cells, Sol. Energy Mater. Sol. Cells 95 (2011) 816–820.
[19] F. Lisco, A. Abbas, J.W. Bowers, G. Claudio, P.M. Kaminski, M. Walls, Electrodeposition of CdTe films on CdS layers deposited using magnetron sputtering and chemical bath deposition, Proceedings of the 10th Photovoltaic Science, Applications and Technology Conference C96 (PVSAT-10), 23–25, Holywell Park, Loughborough University, Loughborough April 2014, pp. 145–148.
[20] K.N. Nithyayini, S.K. Ramasesha, Fabrication of semi-transparent photovoltaic cell by a cost-effective technique, Metall. Mater. Trans. E 2 (2015) 157–163.
[21] T. Miyazaki, A. Akisawa, T. Kashiwagi, Energy savings of office buildings by the use of semi-transparent solar cells for windows, Renew. Energy 30 (2005) 281–304.
[22] J. Pettersson, T. Torndahl, C. Platzer-Bjorkman, A. Hultqvist, M. Edoff, The influence of absorber thickness on Cu (In, Ga) Se solar cells with different buffer layers, IEEE J. Photovoltaics 3 (2013) 1376–1382.
[23] L.A. Kosyachenko, A.I. Savchuk, E.V. Grushko, Dependence of efficiency of thin-film CdS/CdTe solar cell on parameters of absorber layer and barrier structure, Thin Solid Films 517 (2009) 2386–2391.
[24] N. Amin, K. Sopian, M. Konagai, Numerical modeling of CdS/CdTe and CdS/CdTe/ZnTe solar cells as a function of CdTe thickness, Sol. Energy Mater. Sol. Cells 91 (2007) 1202–1208.
[25] Z. Bai, J. Yang, D. Wang, Thin film CdTe solar cells with an absorber layer thickness in micro-and sub-micrometer scale, Appl. Phys. Lett. 99 (2011) 143502(1)–143502(3).
[26] K. Nakamura, M. Gotoh, T. Fujihara, T. Toyama, H. Okamoto, Influence of CdS window layer on 2-μm thick CdS/CdTe thin film solar cells, Sol. Energy Mater. Sol. Cells 75 (2003) 185–192.